Halide Vacancies Created by the Heterogeneous Reaction of OH with Alkali Halide Single Crystals

Matthew A. Brown,[†] Theresa M. McIntire,[†] Viktor Johánek,[‡] and John C. Hemminger*[,†]

Department of Chemistry, University of California, Irvine, California 92697-2025, and Department of Chemistry, University of Virginia, Charlottesville, Virginia 22904-4310

Received: August 30, 2008; Revised Manuscript Received: December 20, 2008

The heterogeneous surface reaction of OH with dry KI(100) results in iodide vacancies in the surface lattice sites that are filled with OH to generate a stable layer of KOH. Under high-vacuum conditions, in which surface ions are not mobile, the reaction is self-passivating and generates two molecular layers of potassium hydroxide, releasing 1.6×10^{16} iodide ions per cm^2 of surface area. Reaction rates are identical with those of NaI(100). A similar surface reaction occurs with alkali bromides (KBr(100)), albeit at a much slower rate to generate approximately one-tenth of a monolayer of KOH, whereas no observable reaction occurs with KCl(100) under the conditions of this experiment. The heterogeneous reaction of OH with alkali halides is found to be dependent solely on the identity of the halide anion and independent of the alkali metal cation with the relative reaction rates following the anion ordering, $I^- > Br^- > Cl^-$. The release of halide-containing species is expected to impact the chemistry of the marine boundary layer.

Introduction

Gas-phase halogens and halogenated oxides affect the composition of the atmosphere, playing a key role in regulating the lifetimes of reactive trace gases.[1−3] Reactions of sea-salt aerosols with gas-phase oxidants (*eg.* ozone and hydroxyl) have been suggested as a source of halogenated species in the marine troposphere.[3−13] Field studies have confirmed the presence of gas-phase halogen compounds in the marine troposphere, verifying these suggestions.[3−6,14−27]

The role of iodide, a minor component of sea-salt aerosol (molar ratio of I^- to Cl^- in seawater is $\sim 1{:}10^6$),[3] in interfacial atmospheric chemistry has recently been questioned following theoretical predictions of increased iodide concentration at the free surface of aqueous saline solutions.[28−31] Spectroscopic measurements have now confirmed the surface propensity of I^- in concentrated aqueous solutions of neat NaI and KI.[32−34] Krisch et al. demonstrated increased ion concentrations at the free surface of more complex ternary systems in which the free surface of KI is covered in a surfactant layer.[35] Studies are now underway to better understand the role of iodide in heterogeneous chemical reactions with implications for atmospheric chemistry. Brown et al. showed the surface of KI(100) to be a sink for ozone, creating an oxidized interface of KIO_3.[36−38] Although the fundamental mechanisms of halogen release are not well understood, heterogeneous reactions that lead to oxidation of the halide components of sea-salt aerosols have been proposed to be responsible for their release in the marine boundary layer, creating photochemically active volatile halogen species.[4]

A number of studies have confirmed the importance of IO and IOI in the chemistry of the marine boundary layer,[17−20] whereas the role of iodide in atmospheric processes is not well understood and continues to be evaluated. Enami et al. recently demonstrated the catalytic activity of iodide in the oxidation and subsequent release of bromine ($Br_{2(g)}$) and chlorine ($Cl_{2(g)}$) in aqueous nanodroplets exposed to ozone.[39] Their study suggests that iodide-containing particles may play a more significant role in the atmosphere through secondary processes than previously recognized.

In this paper, the loss of iodide from the surface of KI(100) following reaction with hydroxyl (OH) radicals in the presence of minimal amounts of water vapor is reported. Hydroxyl radicals (OH) play an important role in the atmosphere by initiating the photooxidation processes of many pollutants. In the reaction processes studied here, the halide vacancies created in the KI lattice are replaced with OH^-, and a passivating layer of KOH is generated. Results from the KI(100) surface are compared with those of NaI(100), KBr(100), and KCl(100) surfaces. The surface composition is monitored using X-ray photoelectron (XP) spectroscopy (XPS), while atomic force microscopy (AFM) is used as a local probe to monitor changes in surface topography.

Experimental Section

Solid samples of alkali halide single crystals (Hilger, U.K., and MaTeck, Germany) were cleaved along the (100) plane and immediately transferred to the XPS vacuum system. The freshly cleaved samples contained small O(1s) intensities in the XP spectra prior to any OH exposure, a result of strongly adsorbed surface water that adsorbs from the gas phase during the cleavage process in ambient air. Hydroxyl radical exposures, produced by photodissociation of a H_2O_2/H_2O gas mixture, were performed with a custom-made dosing system that has been described in detail in the published literature.[40] Exposures herein were performed with a backing pressure of 5.0 mTorr, resulting in a pressure in the photointeraction region in the free molecular flow regime limiting any secondary reactions. Under these conditions, the doser generates an incident flux on the sample surface of $\sim 10^{10}$ OH/sec. The OH flux is uniform across the sample surface to within 5%, and the flux is reproducible from

* To whom correspondence should be addressed. E-mail: jchemmin@uci.edu.
[†] University of California.
[‡] University of Virginia.

10.1021/jp807731s CCC: $40.75
Published on Web 02/11/2009

experiment to experiment to within 10%.[40] Following XPS measurements to monitor the surface elemental composition, samples were transferred to the AFM instrument for subsequent analysis of the surface topography.

XPS experiments were performed with an ESCALAB MKII (VG Scientific) surface analysis instrument. XP spectra presented herein were collected using Mg Kα incident radiation (1253.6 eV). During these experiments the base pressure of the spectroscopy chamber was 1×10^{-9} Torr. The experiments were carried out in constant analyzer energy (CAE) mode at a pass energy of 10 eV. After each OH exposure, XPS peak areas for I(4d), K(2p), Na(1s), Br(3d), Cl(2p), and O(1s) were measured. Peak areas were normalized to the intensity of the freshly cleaved crystal. XPS peak positions were referenced to the $K(2p_{3/2})$ of the original potassium halide(100) starting material (KI, KBr, and KCl) or to the Na(1s) of the original NaI(100) starting material.

Specimens of freshly cleaved KI(100) crystals before and after reaction with OH were imaged in a dry argon environment using a Park Scientific Instruments AutoProbe CP Research scanning probe microscope operating in tapping mode. Highly doped silicon tips (Budget Sensors) with a force constant of 3 N/m were used throughout. The piezoelectric scanner was calibrated using a grating in the *xy* direction and in the *z* direction using several conventional height standards.

Results and Discussion

Narrow region XP spectra of the I(4d) and O(1s) regions are shown in Figure 1 (top and bottom panels, respectively) for the KI(100) system. The freshly cleaved KI(100) surface has a small intensity in the O(1s) region prior to the first OH exposure, attributed to strongly adsorbed water as a result of the cleavage process in ambient laboratory air. As the exposure to OH is increased, a decrease in the I(4d) intensity is observed, while there is an increase in the O(1s) intensity. The increase in the O(1s) intensity is attributed to the reaction of the OH radical with the surface. Under our experimental conditions, with a 5 mTorr backing pressure of a 50% w/w H_2O_2/H_2O aqueous gas mixture and the source photolysis lamps turned off (no OH production), no background reactivity is observed on the single-crystal KI(100) surfaces.

Atomic ratios of the I(4d) and O(1s) to the K(2p) are shown in Figure 2, which summarizes the results of the uptake measurements shown in Figure 1. Initially, a stoichiometric I(4d)/K(2p) ratio is measured. With increasing exposure to OH, a strong O(1s) intensity grows in, while there is a corresponding decrease in the I(4d) intensity (seen in the decrease of the I(4d)/K(2p) atomic ratio). Following prolonged exposures of the KI(100) surface to OH, the surface passivates, and no further increase in O(1s) intensity or decrease in I(4d) intensity is observed.

Binding energies (BE) of the I(4d) and O(1s) atomic orbitals referenced to that of the $K(2p_{3/2})$ are displayed in Figure 3 as the exposure to OH is increased to a KI(100) single crystal. The $K(2p_{3/2})$ BE has been set at 292.8 eV.[41] At all exposures of OH, the I(4d) BE remains constant at 48.9 (±0.15) eV, in agreement with its literature value.[41] At all exposures of OH, there is a single iodide oxidation state in the XP spectra. That is, there is no spectroscopic evidence for the formation of higher oxidation state iodide species during the reaction. The slight shift to a higher binding energy of the O(1s) orbital that is easily seen in Figure 1 is consistent with a nonstoichiometric KOH/KI/KIO_x film that could exist during the initial stages of the reaction evolving to a KOH film as the reaction proceeds to saturation.

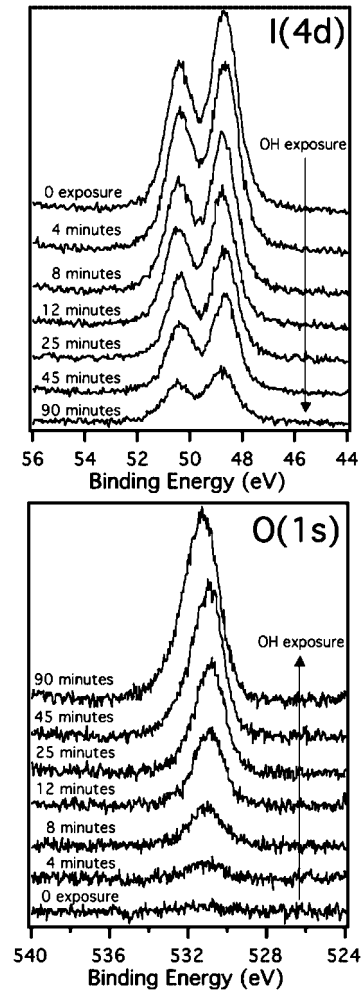

Figure 1. Narrow region XP spectra of the iodide I(4d) (top panel) and O(1s) (bottom panel) regions following various exposures of a single crystal of KI (100) to OH. The binding energy scale is relative to that of $K(2p_{3/2})$ set to 292.8 eV.[41] OH exposures are shown in minutes for an incident flux of $\sim 10^{10}$ OH/sec at the sample surface.

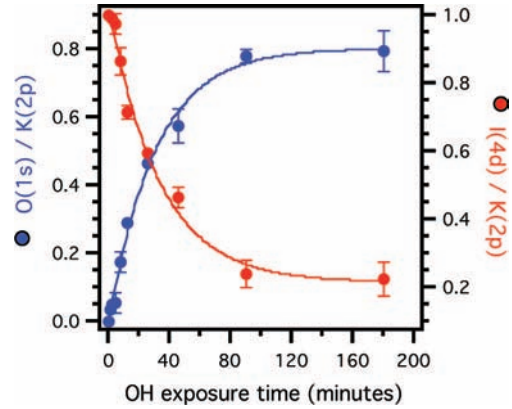

Figure 2. Uptake measurements as a function of OH exposure time onto a KI(100) single-crystal surface. In these experiments, the incident flux of OH at the sample surface was $\sim 10^{10}$ OH/sec. The left axis displays the O(1s)/K(2p) ratio, while the right axis is the I(4d)/K(2p) atomic ratio. Error bars indicate the reproducibility of multiple experiments on newly prepared samples.

At saturation exposures of OH, the underlying I(4d) of the original KI starting material is still present, indicating that the thickness of the passivating KOH layer is less than the probing depth of our XPS experiment (I(4d) photoelectrons were collected at a kinetic energy of ~1200 eV). Under these

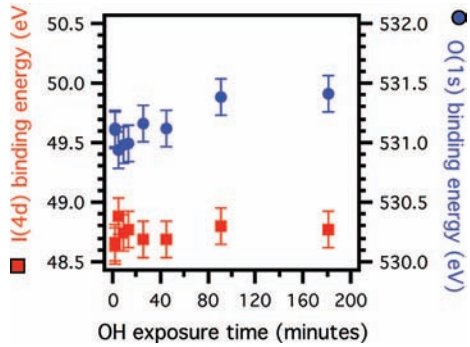

Figure 3. Binding energies (BE) of the I(4d) and O(1s) atomic orbitals as the exposure to OH is increased for a KI(100) surface. BE's are referenced to that of the $K(2p_{3/2})$ set at 292.8 eV.[41] Within the present precision of our measurements, the BE of the I(4d) orbital remains constant at all exposures of OH. The slight shift to higher binding energy of the O(1s) orbital as the exposure to OH is increased is consistent with a nonstoichiometric KOH/KI/KIO_x film that could exist during the initial stages of the reaction evolving to a KOH film as the reaction proceeds to saturation.

conditions, the probe depth is 4.3 nm.[42] The thickness of the KOH layer formed at passivation can be calculated from the decrease in the iodide I(4d) signal using a simple overlayer equation

$$d = \lambda_L \ln(I_o/I_x)$$

where d is the potassium hydroxide layer thickness and λ_L is the attenuation length in KOH, taken to be 4.3 nm for a photoelectron of 1200 eV kinetic energy. I_o is the I(4d) photoelectron peak area of a freshly cleaved KI(100) surface, whereas I_x is the photoelectron intensity of the I(4d) orbital following saturation with OH to form a layer of KOH. A thin 7 Å layer of KOH is formed, corresponding to a loss of ~2 molecular layers of iodide from the KI lattice. For a typical KI(100) sample of 1 cm^2, two molecular layers consist of 1.6×10^{16} I^- ions.[43] Since the reaction occurs over quite a long time scale (~90 min to achieve a passivated surface), the steady-state concentration of the reaction product released into the gas phase is too low for us to detect in our present apparatus. As a result, we are presently unable to identify in which chemical state the iodine is being released (e.g., I_2, IO, IOH, IOI, etc.). The chemical identity of the released iodine has implications in atmospheric chemistry. Bloss et al. recently showed that the HO_2/OH ratio in the coastal marine boundary layer is significantly altered by IO,[16] whereas the condensation of I_2 to form new ultrafine particles in the daytime marine atmosphere has been shown in multiple research laboratories and explored in detail using an iodine chemistry model by Saiz-Lopez.[20] Studies are presently underway in our laboratory to identify the chemical nature of the released iodine species.

We have previously shown that in the absence of water vapor, the heterogeneous reaction of ozone with KI(100) results in oxidation of the iodide-anion-forming iodate, in dramatic contrast to what we observe here for the OH reaction.[37] The passivating layer of KIO_3 formed in the reaction with ozone consists of small particles, 10−30 nm in width and 4−6 nm in height, that are evenly distributed across the sample surface.[36] The reaction does not result in iodide vacancies across the (100) crystal plane, where the total I(4d)/K(2p) atomic ratio remains near unity (ie., $[I^-(4d) + I^{+5}(4d)]/K(2p) \sim 1$).[37]

Figure 4 compares the loss of iodide from the surface of KI(100) with that from the surface of NaI(100) due to the OH reaction studied here. The results are plotted as a ratio of the

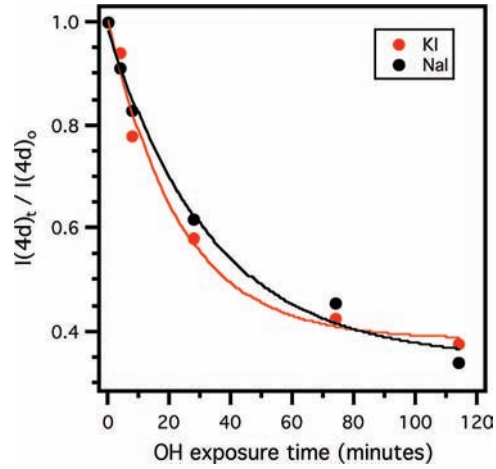

Figure 4. Decrease in surface iodide with increased exposure to OH. The red and black markers are for KI and NaI, respectively. The solid lines are fits to the data. The loss of I^- upon reaction with OH is independent of the cation identity.

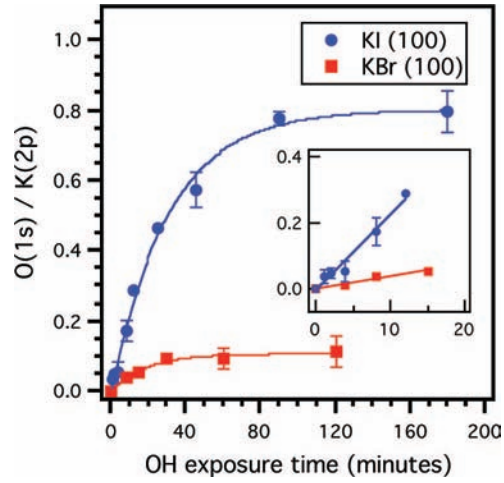

Figure 5. Uptake measurements as a function of OH exposure time comparing the relative rates of reaction with the surfaces of KI(100) and KBr(100). The inset shows the early stages of the reaction in more detail. The initial reaction rate is six times greater for the KI(100) surface than that for the KBr(100) surface. Following prolonged exposures, the KI(100) surface is covered in two molecular layers of KOH, whereas the saturation OH uptake onto KBr(100) results in less than a monolayer of KOH. Error bars indicate the reproducibility of multiple experiments on newly prepared samples.

remaining surface area of the I(4d) orbital to that of the freshly cleaved surface, $I(4d)_t/I(4d)$. Both alkali iodide surfaces react with OH at the same rate, independent of the cation. Following prolonged exposures of OH, the surface of NaI(100) passivates to create a thin layer of NaOH similar to that of the KI(100) system.

Figure 5 compares the relative rates of reaction of OH with the surface of KI(100) and KBr(100) under similar experimental conditions. As can be seen from the short-time exposure data, the initial reaction of OH with KI(100) proceeds at a relative rate six times faster than that with the surface of KBr(100). It is important to note here that we are comparing rates of the reaction with the two single-crystal surfaces not reaction rate constants. Since the concentration of reactive sites may be different on the two surfaces, we do not have a direct way to obtain the rate constants for the reaction of OH with an active site on the two surfaces. Following prolonged exposures of the KBr(100) surface to OH, less than a single molecular layer of KOH is formed, on the order of one-tenth of a monolayer. By

comparison, in the case of KI(100), two complete layers of KOH are formed. As was pointed out previously,[17] it remains difficult to accurately determine a quantitative OH uptake coefficient for these systems. The OH radicals are produced in the molecular flow regime of our high-vacuum doser, making quantification of the OH concentration impinging on the sample surface an experimental challenge. As such, it is much more reliable for us to report relative uptake coefficients for the different alkali halide single-crystal surfaces under similar reaction conditions. It is evident from our experiments that the reactivity of iodide-containing solid surfaces with OH far exceeds that of bromide-containing compounds under the conditions of our experiment, in which the surface is considered to be devoid of adsorbed water molecules. The alkali iodide surface reacts to form two molecular layers of alkali hydroxide, whereas the reaction with the potassium bromide surface saturates after formation of only a submonolayer amount of product. A possible explanation for this difference in saturation coverage is that the reaction with OH on the KBr surface may only occur at step-edge, point defect sites and locations across the samples terraces where small amounts of surface-adsorbed water reside. In contrast, the OH reaction with KI(100) occurs across the entire surface until the multilayer saturation film is formed. Under this mechanism (we are presently unable to carry out an AFM experiment in situ to provide further experimental evidence), the surface of KBr(100) contains, on average, an approximately 10% surface defect density. The surface reaction of KBr(100) with OH studied here is then complete once the surface defect sites have reacted, resulting in one-tenth of a monolayer of KOH reaction product. We should stress that until in situ imaging experiments (e.g., AFM) that we are now designing can be carried out, we do not know for certain that the OH reaction on KBr(100) is limited solely to defect sites or regions with adsorbed water. However, the expected defect density on the KBr(100) surfaces that we used in these experiments is consistent with the one-tenth of a monolayer saturation level.

Additional uptake measurements with KCl(100) were carried out. Under the same reaction conditions to those presented herein, the reaction of OH with KCl(100) results in no measurable uptake of oxygen onto the surface and does not create halide vacancies in the KCl(100) crystal lattice. Figure 6 displays the XP spectra of the K(2p), Cl(2p), and O(1s) atomic orbitals from a KCl(100) single-crystal surface before (red squares) and after (blue solid lines) exposure to 90 min of OH at a surface flux of $\sim 10^{10}$ OH/sec. There is no net change in the O(1s)/K(2p) atomic ratio following exposure to OH (before 0.01; after 0.02; for comparison, the O(1s)/K(2p) atomic ratio from the KI(100) sample prior to exposure was 0.03, and following a similar 90 min OH exposure, it increased to 0.78). The small, albeit measurable O(1s) intensities from the freshly cleaved alkali halide surfaces are a result of strongly adsorbed water at step-edge and defect sites, a result of the cleavage process in ambient laboratory air. There is also no net loss of chloride from the KCl(100) lattice sites following exposure to OH, with an atomic stoichiometry following reaction of 0.99 (well within the reproducibility of our measurements).

Using a flow tube technique combined with an EPR spectrometer as a detection method, Ivanov et al. studied the heterogeneous uptake of OH onto dry NaCl over a temperature range of 245−340 K and found a γ_{NaCl}^{OH} of $(1.2 \pm 0.5) \times 10^{-4}$.[44] Our experiments are consistent with this low reaction probability for this reaction of OH with KCl. The results of their study conclude that the heterogeneous OH sinks on solid NaCl aerosol

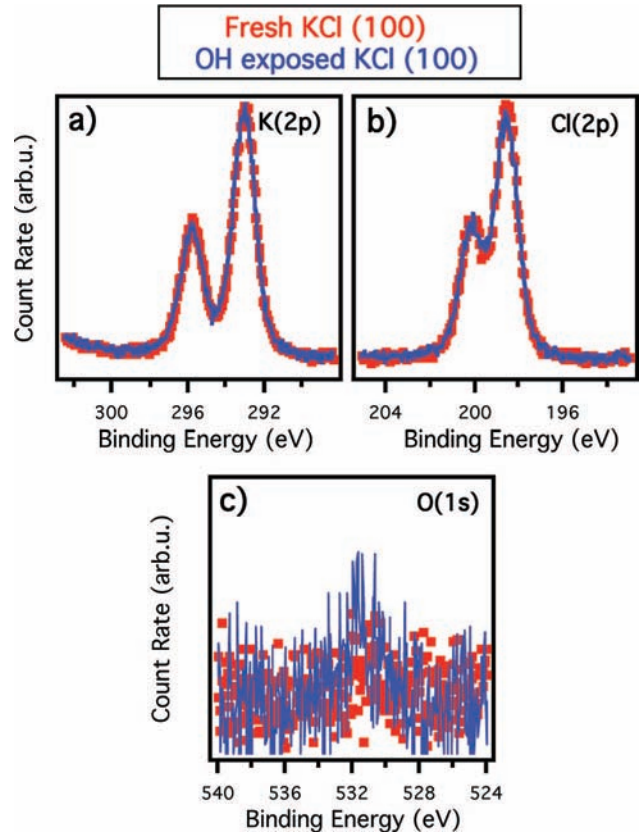

Figure 6. High-resolution XP spectra of the K(2p) (a), Cl(2p) (b), and O(1s) (c) atomic orbitals from a KCl(100) single-crystal surface. The spectra of the freshly cleaved surface are shown as red squares, whereas the solid blue lines were collected following a 90 min exposure to OH at a surface flux of $\sim 10^{10}$ OH/sec. There is no net increase in O(1s) intensity onto the surface. In addition, the chloride to potassium stoichiometry remains unity following reaction, indicating that there is no halide replacement created throughout the KCl lattice with OH exposure.

play a very minor role in tropospheric chemistry in comparison with the homogeneous sinks. The present study has confirmed that the heterogeneous sinks associated with chloride-containing species play a very minor role in comparison to iodide-containing compounds. No study of alkali iodides or bromides was reported in the Ivanov et al. study. The flow tube technique is unable to detect changes in the surface composition such as the surface halide vacancies that we report here. To the best of our knowledge, the present study is the first direct observation of halide replacement created by heterogeneous surface reaction of alkali halides with OH under dry conditions. The heterogeneous reaction of OH with the surface of alkali halides is dependent on the identity of the halide ion and independent of the alkali metal cation, and being a surface-specific reaction, it is expected to scale with exposed halide surface area.

An ex situ AFM image obtained following surface passivation of KOH from a KI(100) single crystal is shown in Figure 7. There are large particles that have formed across the sample terraces that are assigned as KOH. Under ambient laboratory conditions (~35% relative humidity), the surface ions become solvated and mobile. Under these conditions (the sample needed to be transferred between instruments for AFM analysis), the surface KOH layer restructures into large particles as a means to minimize the surface free energy. It is our belief that the surface reconstruction is an artifact induced by surface ionic mobility and would not be present if we were able to monitor the surface topography in situ under high-vacuum conditions.

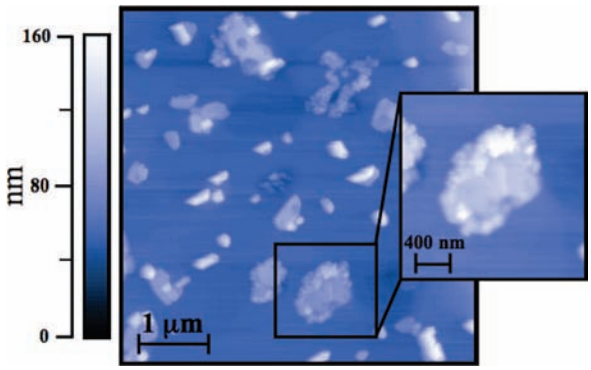

Figure 7. AFM micrograph of the KI(100) surface following reaction with OH. The large crystals are assigned as KOH that has restructured from the KI lattice during transfer to the AFM instrument in ambient laboratory air. The reconstruction of the sample surface is an artifact induced by surface ion mobility. The XPS results clearly point toward the formation of a stable homogeneous KOH multilayer under high-vacuum conditions.

While a detailed understanding of the surface morphology during the reaction in vacuum must await in situ imaging experiments, the results of the XPS analysis point toward the formation of two molecular layers of KOH that are evenly distributed across the sample surface.

Thermodynamically, the reaction of gas-phase OH with potassium halide surfaces is energetically downhill according to the following reactions, where the hypohalous acids are formed as a reaction product in the gas phase[45−47]

$$\begin{aligned} KI_{(s)} + 2OH_{(g)} &\rightarrow KOH_{(s)} + IOH_{(g)} \quad \Delta H_f^\circ = -263\ \text{kJ/mol} \\ KBr_{(s)} + 2OH_{(g)} &\rightarrow KOH_{(s)} + BrOH_{(g)} \quad \Delta H_f^\circ = -168\ \text{kJ/mol} \\ KCl_{(s)} + 2OH_{(g)} &\rightarrow KOH_{(s)} + ClOH_{(g)} \quad \Delta H_f^\circ = -145\ \text{kJ/mol} \end{aligned}$$

with an increasing ΔH_f° going from KI to KBr to KCl. The results of our current study are in accord with this trend. The reactivity of OH was seen to be greatest with KI, generating two stable atomic layers of KOH, followed by KBr, where the initial reaction proceeded at a rate six times slower and the passivated reaction generated only approximately one-tenth of a monolayer of KOH. The reaction of OH with the surface of KCl(100) does not result in a measurable uptake of oxygen onto the surface.

There have been a number of aqueous-phase studies that point to unique interfacial chemistry with certain inorganic species, in particular, the halide series of the present study. In a study of deliquesced NaCl particles with OH, Knipping et al. observed the formation of gas-phase $Cl_{2(g)}$ that was far in excess of the amount expected based solely on the bulk acid catalyzed reaction mechanism.[3,7] On the basis of their experimental observation and accompanying molecular dynamics simulations, Knipping et al. proposed an interfacial reaction mechanism that replaced Cl^- in solution with OH^-, thereby releasing gas-phase $Cl_{2(g)}$

$$2Cl^- + 2OH_{(g)} \rightarrow 2OH^- + Cl_{2(g)}$$

Two intermediate surface "complexes" of $OH\cdot Cl^-$ are postulated to form preceding electron transfer, generating the final products.[7] In this mechanism, the halide species are released from the particle as molecular gas-phase iodine, bromine, and chlorine (for particles containing the different halides), and the hypohalous acids (HOI, HOBr, and HOCl) are not produced in the gas phase.

The reaction of OH with the surface of dry alkali halide single-crystal (100) surfaces could follow either of the two reaction pathways outlined above. In one case (we focus on the discussion of potassium iodide(100) here), iodine is released into the gas phase as hypoiodous acid (HOI), whereas following the second proposed reaction pathway, the iodine is released into the gas phase as molecular $I_{2(g)}$. Both models share a similar fate with regards to the surface of the potassium iodide(100) single crystal. The iodide ions are replaced within the crystal lattice framework with OH to generate a stable self-passivating layer of KOH. Once this layer, which is approximately 7 Å thick, is formed, the reaction terminates, and there is no further evidence for the continued reaction and uptake of OH onto the surface.

Conclusion

The heterogeneous surface reaction of OH with dry alkali iodide (KI and NaI(100)) single-crystal surfaces results in oxidation of the halide and formation of halide vacancies across the top two molecular layers that are replaced by hydroxide to form a stable passivating layer of alkali hydroxide. Similar reaction rates are observed for both KI(100) and NaI(100). The reaction with alkali bromide single-crystal surfaces proceeds eight times slower and occurs only at step-edge and point defects sites across the surface, resulting in approximately one-tenth of a monolayer of alkali hydroxide. No net reaction is observed for NaCl(100) under the same reaction conditions. The heterogeneous surface reaction was shown to depend on the identity of the halide ion while being independent of the cation. Presently, the chemical identity of the released halogen species is unknown; however, our results are consistent with the mechanisms suggested in the literature, both of which predict the production of a surface hydroxide. The results presented herein clearly demonstrate that dry sea-salt aerosol should be considered as a source of atmospheric halogen (in particular, iodide-containing particles) compounds and must be properly accounted for in heterogeneous kinetic models.

Acknowledgment. The *AirUCI* Environmental Molecular Sciences Institute under Grant Number CHE 0431312 from the National Science Foundation supported this work. The authors are indebted to Professor Finlayson-Pitts for constructive suggestions on the manuscript and helpful discussions.

References and Notes

(1) Finlayson-Pitts, B. J.; Pitts, J. N., Jr., *Chemistry of the Upper and Lower Atmosphere*; Academic Press: New York, 2000.
(2) Seinfeld, J. H.; Pandis, S. N. *Atmospheric Chemistry and Physics: From Air Pollution to Climate Change*; Wiley: New York, 1998.
(3) Finlayson-Pitts, B. J. *Chem. Rev.* **2003**, *103*, 4801.
(4) Rossi, M. J. *Chem. Rev.* **2003**, *103*, 4823.
(5) Finlayson-Pitts, B. J.; Hemminger, J. C. *J. Phys. Chem. A* **2000**, *104*, 11463.
(6) Hemminger, J. C. *Int. Rev. Phys. Chem.* **1999**, *18*, 387.
(7) Knipping, E. M.; Lakin, M. J.; Foster, K. L.; Jungwirth, P.; Tobias, D. J.; Gerber, R. B.; Dabdub, D.; Finlayson-Pitts, B. J. *Science* **2000**, *288*, 301.
(8) Laux, J. M.; Hemminger, J. C.; Finlayson-Pitts, B. J. *Geophys. Res. Lett.* **1994**, *21*, 1623.
(9) Perovich, D. K.; Richtermenge, J. A. *J. Geophys. Res., [Oceans]* **1994**, *99*, 16341.
(10) Finlayson-Pitts, B. J.; Livingston, F. E.; Berko, H. N. *Nature* **1990**, *343*, 622.
(11) Anastasio, C.; Newberg, J. T. *J. Geophys. Res., [Atmos.]* **2007**, *112*, D10306.
(12) Frinak, E. K.; Abbatt, J. P. D. *J. Phys. Chem. A* **2006**, *110*, 10456.
(13) George, I. J.; Anastasio, C. *Atmos. Environ.* **2007**, *41*, 543.
(14) Keene, W. C.; Stutz, J.; Pszenny, A. A. P.; Maben, J. R.; Fischer, E. V.; Smith, A. M.; von Glasow, R.; Pechtl, S.; Sive, B. C.; Varner, R. K. *J. Geophys. Res., [Atmos.]* **2007**, *112*, D10S12.
(15) Finley, B. D.; Saltzman, E. S. *Geophys. Res. Lett.* **2006**, *33*, L11809.

(16) Bloss, W. J.; Lee, J. D.; Johnson, G. P.; Sommariva, R.; Heard, D. E.; Saiz-Lopez, A.; Plane, J. M. C.; McFiggans, G.; Coe, H.; Flynn, M.; Williams, P.; Rickard, A. R.; Fleming, Z. L. *Geophys. Res. Lett.* **2005**, *32*, L06814.

(17) Alicke, B.; Hebestreit, K.; Stutz, J.; Platt, U. *Nature* **1999**, *397*, 572.

(18) Allan, B. J.; McFiggans, G.; Plane, J. M. C.; Coe, H. *J. Geophys. Res., [Atmos.]* **2000**, *105*, 14363.

(19) Allan, B. J.; Plane, J. M. C.; McFiggans, G. *Geophys. Res. Lett.* **2001**, *28*, 1945.

(20) Saiz-Lopez, A.; Plane, J. M. C. *Geophys. Res. Lett.* **2004**, *31*, L04112.

(21) Foster, K. L.; Plastridge, R. A.; Bottenheim, J. W.; Shepson, P. B.; Finlayson-Pitts, B. J.; Spicer, C. W. *Science* **2001**, *291*, 471.

(22) Spicer, C. W.; Chapman, E. G.; Finlayson-Pitts, B. J.; Plastridge, R. A.; Hubbe, J. M.; Fast, J. D.; Berkowitz, C. M. *Nature* **1998**, *394*, 353.

(23) Hausmann, M.; Platt, U. *J. Geophys. Res.* **1994**, *99*, 25399.

(24) Tuckermann, M.; Ackermann, R.; Golz, C.; LorenzenSchmidt, H.; Senne, T.; Stutz, J.; Trost, B.; Unold, W.; Platt, U. *Tellus Ser. B* **1997**, *49*, 533.

(25) Platt, U.; Hausmann, M. *Res. Chem. Intermed.* **1994**, *20*, 557.

(26) Kreher, K.; Johnston, P. V.; Wood, S. W.; Nardi, B.; Platt, U. *Geophys. Res. Lett.* **1997**, *24*, 3021.

(27) Osthoff, H. D.; Roberts, J. M.; Ravishankara, A. R.; Williams, E. J.; Lerner, B. M.; Sommariva, R.; Bates, T. S.; Coffman, D.; Quinn, P. K.; Dibb, J. E.; Stark, H.; Burkholder, J. B.; Talukdar, R. K.; Meagher, J.; Fehsenfeld, F. C.; Brown, S. S. *Nat. Geosci.* **2008**, *1*, 324.

(28) Dang, L. X. *J. Phys. Chem. B* **2002**, *106*, 10388.

(29) Dang, L. X.; Chang, T. M. *J. Phys. Chem. B* **2002**, *106*, 235.

(30) Jungwirth, P.; Tobias, D. J. *J. Phys. Chem. B* **2001**, *105*, 10468.

(31) Jungwirth, P.; Tobias, D. J. *Chem. Rev.* **2006**, *106*, 1259.

(32) Petersen, P. B.; Johnson, J. C.; Knutsen, K. P.; Saykally, R. J. *Chem. Phys. Lett.* **2004**, *397*, 46.

(33) Ghosal, S.; Hemminger, J. C.; Bluhm, H.; Mun, B. S.; Hebenstreit, E. L. D.; Ketteler, G.; Ogletree, D. F.; Requejo, F. G.; Salmeron, M. *Science* **2005**, *307*, 563.

(34) Brown, M. A.; D'Auria, R.; Kuo, I.-F. W.; Krisch, M. J.; Starr, D. E.; Bluhm, H.; Tobias, D. J.; Hemminger, J. C. *Phys. Chem. Chem. Phys.* **2008**, *10*, 4778.

(35) Krisch, M. J.; D'Auria, R.; Brown, M. A.; Starr, D. E.; Bluhm, H.; Tobias, D. J.; Hemminger, J. C. *J. Phys. Chem. C* **2007**, *111*, 13497.

(36) Brown, M. A.; Ashby, P. D.; Ogeltree, D. F.; Salmeron, M.; Hemminger, J. C. *J. Phys. Chem. C* **2008**, *112*, 8110.

(37) Brown, M. A.; Newberg, J. T.; Krisch, M. J.; Mun, B. S.; Hemminger, J. C. *J. Phys. Chem. C* **2008**, *112*, 5520.

(38) Brown, M. A.; Liu, Z.; Ashby, P. D.; Mehta, A.; Grimm, R. L.; Hemminger, J. C. *J. Phys. Chem. C* **2008**, *112*, 18287.

(39) Enami, S.; Vecitis, C. D.; Cheng, J.; Hoffmann, M. R.; Colussi, A. J. *J. Phys. Chem. A* **2007**, *111*, 8749.

(40) Brown, M. A.; Johánek, V.; Hemminger, J. C. *Rev. Sci. Instrum.* **2008**, *79*, 02410.

(41) Morgan, W. E.; Stec, W. J.; Vanwazer, J. R. *J. Am. Chem. Soc.* **1973**, *95*, 751.

(42) Powell, C. J.; Jablonski, A. *NIST Electron Inelastic-Mean-Free-Path Database*, Version 1.1; National Institute of Standards and Technology: Gaithersburg, MD, 2000.

(43) Hambling, P. G. *Acta Crystallogr.* **1953**, *6*, 98.

(44) Ivanov, A. V.; Gershenzon, Y. M.; Gratpanche, F.; Devolder, P.; Sawerysyn, J. P. *Ann. Geophys.* **1996**, *14*, 659.

(45) Lide, D. R. *Handbook of Chemistry and Physics*; CRC Press: Cleveland, OH, 2004.

(46) Espinosa-Garcia, J. *Chem. Phys. Lett.* **1999**, *315*, 239.

(47) Ruscic, B.; Berkowitz, J. *J. Chem. Phys.* **1994**, *101*, 7795.

JP807731S